Photoionization from the $6p\ ^2P_{3/2}$ state of neutral cesium

S. U. Haq* and Ali Nadeem
National Institute of Lasers and Optronics (NILOP), P. O. Box Nilore, Islamabad 45650, Pakistan
(Received 12 May 2010; published 30 June 2010)

We report the photoionization studies of cesium from the $6p\ ^2P_{3/2}$ excited state to measure the photoionization cross section at and above the first ionization threshold, oscillator strength of the highly excited transitions, and extension in the Rydberg series. The photoionization cross section at the first ionization threshold is measured as 25 (4) Mb and at excess energies 0.02, 0.04, 0.07, and 0.09 eV as 21, 19, 17, and 16 Mb, respectively. Oscillator strength of the $6p\ ^2P_{3/2} \rightarrow nd\ ^2D_{5/2}$ ($23 \leqslant n \leqslant 60$) Rydberg transitions has been extracted utilizing the threshold value of photoionization cross section and the recorded $nd\ ^2D_{5/2}$ photoionization spectra.

DOI: 10.1103/PhysRevA.81.063432 PACS number(s): 32.80.Fb, 32.80.Rm

I. INTRODUCTION

We present here the results of the photoionization from the low-lying excited states of cesium. This experimental work provides information on the spectroscopically important parameters such as the photoionization cross section of the excited state, level energies, and oscillator strength of the Rydberg transitions. The accurate knowledge of these parameters is valuable for determining the abundance of elements in stellar atmosphere; astrophysicists are interested (in these parameters) for analyzing the composition and temperature of stars and for understanding the processes in plasma.

Photoionization cross section from the ground state and from the excited states of cesium has been investigated theoretically and experimentally. The theoretical [1–3] as well as experimental [4–6] photoionization cross sections from the ground state have been reported, but relatively little data have been available from the $6p\ ^2P_{3/2}$ excited state of cesium. Weisheit [7] calculated the partial photoionization cross sections of the $6p\ ^2P_{1/2,3/2}$ excited states of cesium at various energies near the ionization threshold, incorporating the spin-orbit perturbation and the polarization interaction of valence electrons with the core. The wavelength (λ) dependence of the cross section from $6p\ ^2P_{1/2,3/2}$ states was investigated by Nygaard *et al.* [8], revealing λ^2 dependence at threshold and λ^4 dependence at lower wavelengths. Gerwert and Kollath [9] measured the photoionization cross section from the $7\ ^2P_{3/2}$ and $6\ ^2D_{3/2}$ excited states deep in the continuum at various energy positions. Measurements of the photoionization cross section of the $6p\ ^2P_{3/2}$ state of cesium using cold atoms were reported by Marago *et al.* [10], Patterson *et al.* [11], and Arimondo *et al.* [12] at different energy positions in the above threshold region and compared their results with the earlier theoretical and experimental data. In the present contribution, the absolute photoionization cross section from the $6p\ ^2P_{3/2}$ excited state was measured at the ionization threshold and in the above threshold region at four energies; the results were compared with the previously reported data.

The earliest measurements of the level energies of cesium are mainly based on classical absorption spectroscopy techniques [13–15]. Most of the investigations for the highly excited states of cesium are based on two-photon excitation from the ground state. Popescu *et al.* [16] observed the $n\ ^2S_{1/2}$ ($11 \leqslant n \leqslant 14$) and the $n\ ^2D_{5/2,3/2}$ ($9 \leqslant n \leqslant 13$) Rydberg states. Niemax and Weber [17] reported the fine-structure splitting of the $n\ ^2D_{5/2,3/2}$ levels ($18 \leqslant n \leqslant 23$) using the Doppler free two-photon excitation technique in conjunction with a thermionic dido ion detector and a part of the saturation spectrum of Cs_2 band was also observed. Lorenzen *et al.* [18] reported the term energies of the $n\ ^2D_{3/2}$ ($11 \leqslant n \leqslant 44$), $n\ ^2D_{5/2}$ ($11 \leqslant n \leqslant 44$), and $ns\ ^2S_{1/2}$ ($12 \leqslant n \leqslant 35$) states of cesium via Doppler free two-photon spectroscopy. Utilizing same scheme, O'Sullivan and Stoicheff [19] further extended the $6\ ^2S_{1/2} \rightarrow nd\ ^2D_{3/2,5/2}$ series up to $n = 50$ and $n = 53$, respectively. Weber and Sansonetti [20] used nonresonant and resonantly enhanced Doppler free two-photon spectroscopy for the measurements of absolute energies of the $n\ ^2S_{1/2}$, $n\ ^2P_{1/2}$, $n\ ^2D_{5/2}$, $n\ ^2F_{5/2}$, and $n\ ^2G_{7/2}$ states. Pendrill *et al.* [21] extended the photoexcitation spectra of the $n\ ^2P_{1/2,3/2}$ ($20 \leqslant n \leqslant 60$), $n\ ^2D$ ($54 \leqslant n \leqslant 58$), $n\ ^2F$ ($23 \leqslant n \leqslant 109$), and $n\ ^2G$ ($27 \leqslant n \leqslant 36$) Rydberg states and Riamond *et al.* [22] reported the quantum defects of the *nS*, *nP*, *nD*, and *nF* series. The above literature survey show that most of the available data on the $nd\ ^2D_{3/2,5/2}$ states are based on the Doppler free two-photon spectroscopy, excited from the ground state. We have measured the term energies and the quantum defects of the $6p\ ^2P_{3/2} \rightarrow nd\ ^2D_{5/2}$ transitions using stepwise excitation technique and extended the $nd\ ^2D_{5/2}$ transitions up to $n = 65$.

As the studies of the Rydberg states are mainly focused on the two-photon transitions from the ground state, the oscillator strength of the cesium transitions are limited to the principal series and to the low-lying transitions [23–28]. Fabry [27] reported the *f* values of the principal series and of various excited transitions taking into account the effect of atomic core polarization. Thereafter, Fabry and Cussenot [28] determined the oscillator strength, theoretically as well as experimentally, of the principal series and of the transitions among the *ns*, *np*, *nd*, and *nf* series. Lahiri and Manson [29] calculated the oscillator strength among the ground state and the *s*, *p*, *d*, and *f* excited states (up to $n = 9$) and compared their results with the experimental and the semiempirical results. Recently, Tojo *et al.* [30] used a temperature-controlled cell and a diode laser for the measurement of quadrupole oscillator strength of the $6\ ^2S_{1/2} \rightarrow 5\ ^2D_{5/2}$ transition of cesium as $(4.69 \pm 0.05) \times 10^{-7}$. In the present work the oscillator strength of the $6p\ ^2P_{3/2} \rightarrow nd\ ^2D_{5/2}$ ($23 \leqslant n \leqslant 60$) Rydberg transitions have been determined

*Corresponding author: sami_ulhaq2002@yahoo.com

incorporating the measured value of the photoionization cross section at the first ionization threshold.

II. EXPERIMENTAL DETAILS

The experimental setup used for the photoionization studies is similar as described in our earlier work [31,32]. Briefly, the laser system was composed of a *Q*-switched Nd:YAG laser (30-Hz repetition rate and 7 ns pulse duration). The second (532 nm) and third (355 nm) harmonics were used to pump two Hanna-type dye lasers [33]. The linewidth of the dye lasers was $\leqslant 0.3\ \mathrm{cm}^{-1}$. The first dye laser, charged with LDS 820 dye, was pump by the second harmonic and was fixed at 852.3 nm, which corresponds to the $6s\ ^2S_{1/2} \rightarrow 6p\ ^2P_{3/2}$ transition of cesium. The second dye laser charged with coumarin 500 dye which was pumped by a third harmonic of the same Nd:YAG laser was scanned from 19407 to 19680 cm^{-1} and the $6p\ ^2P_{3/2} \rightarrow nd\ ^2D_{5/2}$ Rydberg series was recorded. Both the exciting and scanning dye laser beams were fed into the thermionic diode from opposite sides and their spatial overlap was ensured in the central region.

The cesium vapors were confined in a heat pipe oven, operating as a thermionic diode ion detector working in space-charge-limited mode. The heat pipe consists of a cylindrical stainless steel tube, 48 cm long, and has an internal diameter of 3 cm and both ends were sealed with the quartz windows. A 0.25-mm-thick molybdenum wire was stretched axially along the tube which acts as cathode and was heated by a separate regulated power supply. The central heating zone (≈20 cm) was heated up to 500 K ± 1% and was monitored by a Ni-Cr-Ni thermocouple. The system was evacuated down to 10^{-5} mbar and about 1 g of cesium in a stainless steel boat was placed in the middle of the heat pipe. The heat pipe was then filled with argon pressure of ≈3–4 mbar to reduce vapor diffusion and to protect the windows. The change in the diode current due to the photo-ion production was measured as a voltage drop across the 100-kΩ load resistor.

For wavelength calibration, a small portion (≈5%) of the scanning laser light was fed into the neon-filled hollow cathode lamp to record the optogalvanic spectrum and another small fraction was passed through a 1-mm-thick solid etalon with a 3.33 cm^{-1} free spectral range and was recorded through photodiode. These signals were recorded simultaneously using three boxcar averagers (*SR-250*), interfaced through a GPIB card (NI 488). The data were recorded and stored on the computer for subsequent analysis. The level energies were determined using a subroutine that takes into account the neon reference wavelengths and the interference fringes from the etalon and yield the energies of all the unknown levels.

The photoionization cross section from the $6p\ ^2P_{3/2}$ excited state was measured using two-step excitation scheme at and above the ionization threshold. The first dye laser (exciting laser) was fixed at the $6p\ ^2P_{3/2}$ state (852.3 nm) and the second dye laser (ionizing laser) was fixed at the first ionization threshold (508.3 nm) and at four energy position (505, 500.2, 495, and 490 nm) above the ionization threshold. The ionizing laser beam was focused to a diameter, smaller than that of the exciting laser beam and their energy was measured by the energy meter (3Sigma, Coherent). The intensity of the ionizing laser beam was varied using the neutral density filters and the photoionization signals were registered on a storage oscilloscope at each value of the ionizing laser beam energy.

III. RESULTS AND DISCUSSION

In the present work, we have measured the absolute value of threshold photoionization cross section from the $6p\ ^2P_{3/2}$ excited state of cesium by employing the saturation technique as described by Burkhardt *et al.* [34]. This technique has been widely used for the measurement of photoionization cross section from the excited states of alkali metals and alkaline-earth metals [35–40]. In this technique, the atoms are excited to the desired state and from there these atoms are ionized via second laser tuned either to threshold or to any higher energy position. The intensity of the first laser is kept sufficiently high to saturate the transition and the second laser intensity is varied using the neutral density filters and ion yield is recorded at each insertion. Solution of the rate equations for two-step photoionization process gives an expression for the number of ions produced per unit volume. This expression is used to measure the absolute photoionization cross section at a particular wavelength of the ionizing laser:

$$Z = \frac{Q}{eV_{\mathrm{vol}}} = N_0\left[1 - \exp\left(-\frac{\sigma U}{2\hbar\omega A}\right)\right]. \tag{1}$$

Here Z is the total number of ions collected per unit volume, e (coulomb) is the electric charge, N_0 (cm^{-3}) is the density of excited atoms, U (joule) is the total energy per ionizing laser pulse, $h\omega$ (joule) is the energy per photon of the ionizing laser beam, V_{vol} (cm^3) is the laser interaction volume, σ (cm^2) is the cross section for photoionization, and A (cm^2) is the cross sectional area of the ionizing laser beam. The accurate measurement of the ionizing laser energy and the characterization of a spatial beam profile of the exciting and the ionizing lasers are the two major factors for accurate measurement of the photoionization cross section. The laser beams were scanned across the photodiode and their intensity distribution was Gaussian. The spot sizes of these beams were determined at the point where the irradiance (intensity) falls to $1/e^2$ of their axial (peak) value. In the two-step photoionization, the atoms from the $6s\ ^2S_{1/2}$ ground state of cesium were promoted to the $6p\ ^2P_{3/2}$ state via first dye laser tuned at 852.3 nm and the second dye laser was fixed at the $^1S_0$ threshold and at various energy positions in the continuum. At each ionizing laser wavelength, the dye laser intensity was varied by inserting the neutral density filters in their path and was measured by an energy meter. We have registered the signal intensities against the pulse energies of the ionizing laser beam on a storage oscilloscope. In order to record the actual photoionization signals, the linearity of the thermionic diode ion detector was made sure by configuring it for the strongest signal. The plot of the photoionization signal versus ionizing laser energy from the $6p\ ^2P_{3/2}$ excited state at the first ionization threshold is shown in Fig. 1. This figure show that the photoion signal first increases to a certain value of ionizing laser intensity and thereafter the slope decreases but could not approached zero value, which is a point of full saturation. The solid line passing through the experimental data points is the least-squares fit of Eq. (1), which yields the photoionization cross section from the $6p\ ^2P_{3/2}$ excited state at the first

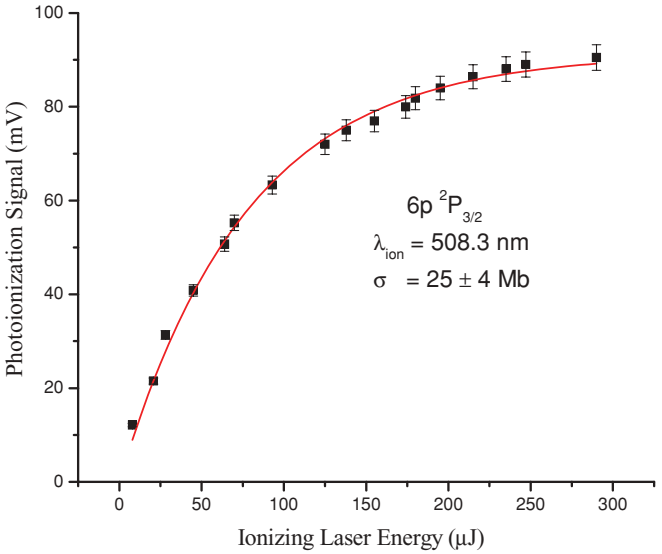

FIG. 1. (Color online) The experimental data points showing the photoionization yield plotted against the ionizing laser intensity. The solid line represents the least-squares fit of Eq. (1). The absolute value of the cross section σ (Mb) from the $6p\ ^2P_{3/2}$ excited state at a 508.3 nm ionizing laser wavelength is extracted as 25 ± 4 Mb. The errors on the data point show pulse-to-pulse variation in the photoionizing signal.

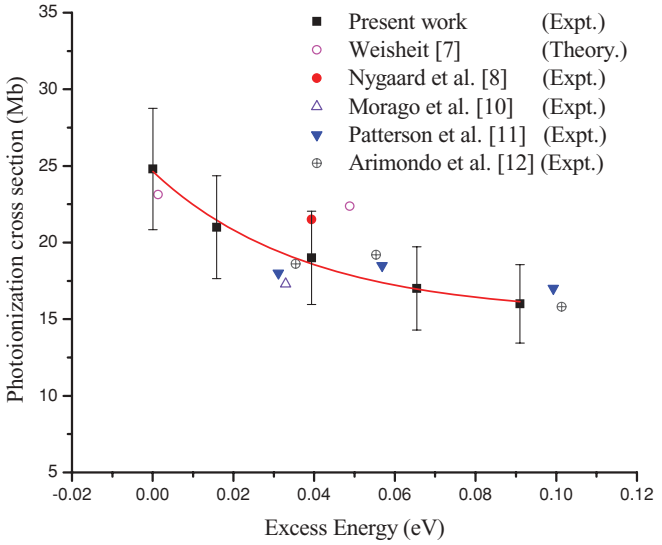

FIG. 2. (Color online) Dependence of the photoionization cross section from the $6p\ ^2P_{3/2}$ excited state of cesium on the excess energy and comparison with the earlier reported work. The solid line which passes through the experimental data points represents the first order exponential decay law.

ionization threshold as 25 ± 4 Mb. The estimated uncertainty in the measurement of photoionization cross section is about 16%, which includes the uncertainty in the measurement of ionizing laser energy, measurement of laser beam diameter, transmission of the quartz windows and in the signal amplitude measurements. As experimental data of the photoionization cross section from the $6p\ ^2P_{2/3}$ excited state of cesium at the first ionization threshold is not available in the literature, we are unable to compare our results. However, the theoretical photoionization cross section at the ionization threshold lies in the 18- to 24-Mb range as reported in Refs. [4,6,7,29,41].

In addition, we have measured the photoionization cross section from the $6p\ ^2P_{3/2}$ excited state at different energy positions in the above threshold region. The extracted photoionization cross sections are 21, 19, 17, and 16 Mb at excess laser energies 0.02, 0.04, 0.07, and 0.09 eV, respectively. In Fig. 2 the photoionization cross section has been plotted against the excess energies, the solid line is the fit of first-order exponential decay expression to the experimental data points, indicating smooth falling trend. It is apparent from this figure that the photoionization cross section is higher in the vicinity of ionization threshold and thereafter decreases smoothly with the increase in energy as predicted theoretically [4,6,7,29,42]. The earlier work (see Fig. 2) of Nygaard *et al.* [8] and Weisheit [7] is represented by closed and open circles, respectively. These results are in agreement within the uncertainty except the one reported by Weisheit [7] at 0.049 eV. At energies greater than 0.03 eV; the cross section measured utilizing the cold atoms have been represented by closed triangles, open triangles, and crossed circles [10–12]. Our results are in close agreement within the uncertainty to the reported data. It is worth mentioning that the smooth decreasing trend in cross section in the near threshold region as shown in Fig. 2 and the $1/n^{2.65}$ scaling trend in intensities of the $nd\ ^2D_{5/2}$ Rydberg series in the bound region clearly discards the existence of Cooper minima. Furthermore, the phase difference between the $6p\ ^2P_{3/2}$ state and threshold (εd) is more than 0.5π [29], which also indicates that no Cooper minima exist in the near threshold region. However, Msezane and Manson [42] and Saha [43] predicted the Cooper minima in ^2D states at higher energies ($\sim$13 eV) in continuum as compared to the present measurements done from 0.02 to 0.09 eV excess energy. It will be interesting to experimentally investigate the photoionization cross section across the location of theoretically predicted Cooper minima.

The photoionization spectra of cesium have been recorded covering the laser energy region from 19407 cm^{-1} to 19680 cm^{-1} excited from the intermediate $6p\ ^2P_{3/2}$ state. The lifetime of the $6p\ ^2P_{3/2}$ state is 30.57 ns [44]. The pulse duration of the second dye laser was 7 ns; therefore, the time delay between the two dye lasers was not very critical. The higher members of the Rydberg series up to the first ionization threshold are shown in Fig. 3. In the *LS*-coupling scheme the accessible series from the intermediate state are $nd\ ^2D_{5/2}$ and $ns\ ^2S_{1/2}$. Therefore, following these selection rules; the dominating series has been assigned as $nd\ ^2D_{5/2}$ ($23 \leqslant n \leqslant 65$), whereas the relatively lower intensity transitions are assigned as $ns\ ^2S_{1/2}$ ($25 \leqslant n \leqslant 45$). The quantum defects associated with each state has been calculated using the Rydberg relation:

$$En = V_{\text{ion}} - \frac{R_{yd}}{(n - \mu_\ell)^2}. \tag{2}$$

Here R_{yd} is the Rydberg constant of cesium 10 9736.862 cm^{-1}, E_n is the energy of the Rydberg level, V_{ion} is the ionization potential 31406.7 cm^{-1}, and μ_ℓ is the quantum defect. The quantum defects of the Rydberg series do not show any variations as a function of the principal quantum number n. The quantum defects determined from the higher member

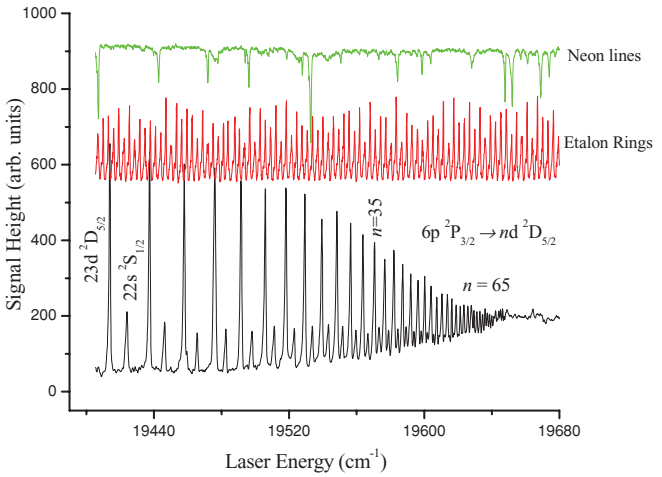

FIG. 3. (Color online) Scan of the $6p\ ^2P_{3/2} \rightarrow nd\ ^2D_{5/2}/\ ns\ ^2S_{1/2}$ Rydberg series, obtained through stepwise excitation from the ground state. The higher-intensity signals are the $nd\ ^2D_{3/2}$ series, whereas the lower-intensity transitions are assigned as $ns\ ^2S_{1/2}$ states.

of the series are also consistent with those calculated from the lower members. The term energies of the observed series have been determined by adding the laser excitation energies to the $6p\ ^2P_{3/2}$ intermediate state energy 11732.35 cm^{-1} [45]. The excited states of cesium have been less thoroughly studied in comparison with other alkali metals and most of the available data on the highly excited states are acquired through two-photon excitation from the ground state. Lorenzen *et al.* [18] reported the higher members of the $nd\ ^2D_{5/2}$ series up to $n = 44$. Subsequently, O'Sullivan and Stoicheff [19] further extended the work by investigating the $nd\ ^2D_{5/2}$ series up to $n = 53$. Weber and Sansonetti [20] also contributed and reported the $n\ ^2D_{5/2}$ states up to $n = 36$ with improved accuracy (0.0002 cm^{-1}). In the present experimental work, the $nd\ ^2D_{5/2}$ series has been extended up to $n = 65$, the results have been compared with the earlier data and are in good agreement within the ± 0.05 cm^{-1} uncertainty. The higher member of the series are used the extract the signal intensities, wavelengths and full width at half maximum (FWHM) of each transition for onward use in determination of oscillator strengths for the corresponding transitions.

The optical oscillator strength for the Rydberg transitions of cesium have been determined by the technique developed by Mende and Kock [46] and widely used for alkalis, alkaline earths, and inert gases [47–50]. A relation is obtained among the f value of a Rydberg transition, the photoionization cross section at threshold, and the wavelength of a particular transition as:

$$f_n = 3.77 \times 10^5 \left(\frac{S_n}{S_{1+}}\right)\left(\frac{\nu_n}{\nu_{1+}}\right)\sigma. \qquad (3)$$

In this expression, f_n is the oscillator strength of a transition, σ is the photoionization cross section measured at the ionization threshold at a frequency ν_{1+}, S_{1+} is the ion signal at the ionization threshold, S_n is the integrated signal intensity, and ν_n is the frequency of the corresponding transition. This technique utilizes the absolute value of photoionization cross section at threshold and the parameters extracted from the recorded Rydberg series. This technique is applicable to the

TABLE I. The f values of the Rydberg transitions along with the term energies (cm^{-1}) and the principal quantum number of the $6p\ ^2P_{3/2} \rightarrow nd\ ^2D_{5/2}$ transitions of cesium.

			$6p\ ^2P_{3/2} \rightarrow nd\ ^2D_{5/2}$ f values	
n	Term energy	Present	Theoretical results Fabry and Cussenot [28]	Experimental results Fabry and Cussenot [28]
5			1.91×10^{-1}	
6			3.35×10^{-1}	
7			9.51×10^{-2}	
8			4.07×10^{-2}	
9			2.15×10^{-2}	
10			1.29×10^{-2}	
11			8.38×10^{-3}	
12				
13				
14				
15				2.4×10^{-3}
16				1.6×10^{-3}
17				1.2×10^{-3}
18				8.3×10^{-4}
19				5.7×10^{-4}
20				
21				
22				
23	31 146.49	1.24×10^{-4}		
24	31 169.95	1.17×10^{-4}		
25	31 190.50	1.03×10^{-4}		
26	31 208.45	9.90×10^{-5}		
27	31 224.03	8.87×10^{-5}		
28	31 238.46	7.57×10^{-5}		
29	31 250.74	7.42×10^{-5}		
30	31 261.80	7.05×10^{-5}		
31	31 271.83	6.00×10^{-5}		
32	31 280.69	6.28×10^{-5}		
33	31 288.79	5.26×10^{-5}		
34	31 296.13	4.87×10^{-5}		
35	31 302.95	4.43×10^{-5}		
36	31 309.02	3.91×10^{-5}		
37	31 314.49	4.11×10^{-5}		
38	31 319.70	3.39×10^{-5}		
39	31 324.41	2.95×10^{-5}		
40	31 328.52	2.90×10^{-5}		
41	31 332.63	3.04×10^{-5}		
42	31 336.25	2.58×10^{-5}		
43	31 339.78	2.39×10^{-5}		
44	31 342.88	2.16×10^{-5}		
45	31 345.87	2.17×10^{-5}		
46	31 348.61	2.11×10^{-5}		
47	31 351.19	1.90×10^{-5}		
48	31 353.71	1.72×10^{-5}		
49	31 355.87	1.55×10^{-5}		
50	31 358.04	1.53×10^{-5}		
51	31 360.24	1.49×10^{-5}		
52	31 361.79	1.29×10^{-5}		
53	31 363.57	1.15×10^{-5}		
54	31 365.34	1.27×10^{-5}		
55	31 366.88	1.24×10^{-5}		
56	31 368.43	1.03×10^{-5}		

TABLE I. *(Continued.)*

n	Term energy	$6p\ ^2P_{3/2} \rightarrow nd\ ^2D_{5/2}$ f values: Present	Theoretical results Fabry and Cussenot [28]	Experimental results Fabry and Cussenot [28]
57	31 369.73	1.13×10^{-5}		
58	31 371.03	8.83×10^{-6}		
59	31 372.30	8.21×10^{-6}		
60	31 373.63	7.23×10^{-6}		
61	31 374.62			
62	31 375.56			
63	31 376.40			
64	31 377.43			
65	31 378.72			

transitions for which the ionization probability approaches unity, therefore, in the present studies only those transitions are considered which lie within KT (where K is the Boltzmann constant and T is the temperature in Kelvin).

We have determined the oscillator strength of the $6p\ ^2P_{3/2} \rightarrow nd\ ^2D_{5/2}$ ($23 \leqslant n \leqslant 60$) transitions of cesium using the measured value of the photoionization cross section at threshold (25 Mb). Table I contain the f values of the above-mentioned Rydberg transitions along with the principal quantum number n and the term energies of the Rydberg states. This table also contains the f values of the previously reported data. The lower limit on the f values is imposed due to the limitation of the technique, which is applicable to the transitions for which the ionization probability approaches to unity. At 500 K operating temperature, the transitions having $n > 23$ lie within kT (344 cm^{-1}) and their collisional ionization probability approaches unity. At higher n, the signal to noise ratio limit the f values at $n = 60$, although term energies have been reported up to $n = 65$. The uncertainty in the determination of the oscillator strength is estimated less than 20%, of which the main contribution (≈16%) is from the measurement of the photoionization cross section. Additional uncertainty is due to the measurement of the signal intensity, FWHM, and the energy position of each Rydberg transition.

We present data on the oscillator strengths of the higher members of the $6p\ ^2P_{3/2} \rightarrow nd\ ^2D_{5/2}$ transitions of cesium. A few groups have reported the oscillator strengths of the lower transitions [23–28]. Fabry and Cussenot [28] reported both theoretical and experimental oscillator strengths of the lower transitions originating from the $6p\ ^2P_{3/2}$ excited state. Figure 4 illustrates the present and the previously reported f values of the $6p\ ^2P_{3/2} \rightarrow nd\ ^2D_{5/2}$ transitions. The closed squares represent the present work which is extended to $n = 60$, whereas the closed circles ($5 \leqslant n \leqslant 11$) are the theoretical

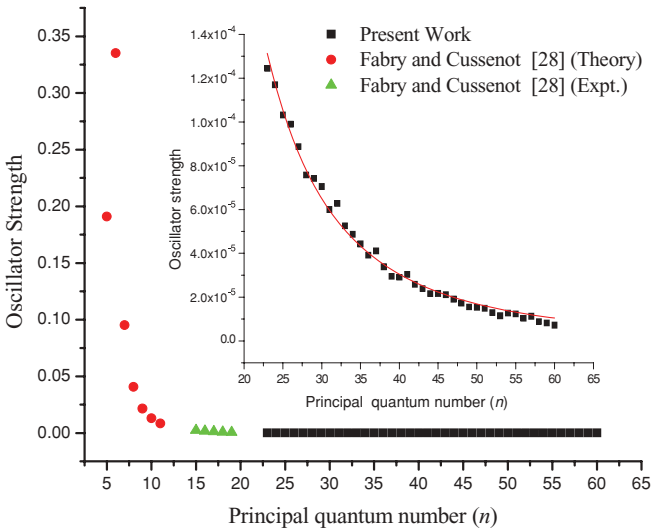

FIG. 4. (Color online) Plot of the oscillator strength distribution in the discrete region versus the principal quantum number (n). The lower n data are taken from Fabry and Cussenot [28] and compared with the present f values. The inserted figure illustrates the trend of the f values with increasing principal quantum number and varies as $1/n^{2.65}$.

results and triangles ($15 \leqslant n \leqslant 19$) represent the experimental f values reported by Fabry and Cossent [28]. The insert in Fig. 4 shows a plot of the currently determined f values versus the principal quantum number n, indicating that the f values of an unperturbed Rydberg series scales as $1/n^{2.65}$. This figure shows a slight variation at the higher n side which may be attributed to variations in the intensities of the spectral lines that subsequently affect the f values of the transitions. This figure provides the overall trend of the f values; however, it will be interesting to cover the gap from $n = 12$–20 using theoretical or experimental technique.

In conclusion, the photoionization cross section from the $6p\ ^2P_{3/2}$ state has been measured in the near-threshold region, revealing a smooth decreasing trend. We have extended the $nd\ ^2D_{5/2}$ ($23 \leqslant n \leqslant 65$) Rydberg series and the f values of the $6p\ ^2P_{3/2} \rightarrow nd\ ^2D_{5/2}$ transitions have been reported up to $n = 60$. This work will be extended to experimentally investigate the minima in cross section as predicated in n^2D states of cesium.

ACKNOWLEDGMENTS

Authors are indebted to Professor M. A. Baig at Quaid-i-Azam University (Islamabad, Pakistan) for valuable suggestions and providing key references. We are also thankful to the Pakistan Atomic Energy Commission (PAEC) for financial support.

[1] G. V. Marr and D. M. Creek, Proc. R. Soc. London A **304**, 233 (1968).
[2] T. B. Cook, F. B. Dunning, G. W. Foltz, and R. F. Stebbings, Phys. Rev. A **15**, 1526 (1977).
[3] K. Grattan, M. Hutchinson, and E. Theocharous, J. Phys. B: Atom. Mol. Phys. **13**, 2931 (1980).
[4] D. W. Norcross, Phys. Rev. A **7**, 606 (1973).
[5] J. C. Weisheit, Phys. Rev. A **5**, 1621 (1972).

[6] D. Hofsaess, Z. Physik **281**, 1 (1977).
[7] J. C. Weisheit, J. Quant. Spectros. Radiat. Transfer **12**, 1241 (1972).
[8] K. J. Nygaard, R. E. Hebner Jr., J. D. Jones, and R. J. Corbin, Phys. Rev. A **12**, 1440 (1975).
[9] K. Gerwert and K. J. Kollath, J. Phys. B: Atom. Mol. Phys. **16**, L217 (1983).
[10] O. Marago, D. Ciampini, F. Fuso, E. Arimondo, C. Gabbanini, and S. T. Manson, Phys. Rev. A **57**, R4110 (1998).
[11] B. M. Patterson, T. Takekoshi, and R. J. Knize, Phys. Rev. A **59**, 2508 (1999).
[12] E. Arimondo, D. Ciampini, F. Fuso, and C. Gabbanini, Appl. Surf. Sci. **154–155**, 527 (2000).
[13] H. R. Kratz, Phys. Rev. **75**, 1844 (1949).
[14] C. J. Sansonetti, K. L. Andrew, and J. Verges, J. Opt. Soc. Am. **71**, 423 (1981).
[15] H. Kleiman, J. Opt. Soc. Am. **52**, 441 (1962).
[16] D. Popescu, C. B. Collins, B. W. Johnson, and I. Popescu, Phys. Rev. A **9**, 1182 (1974).
[17] K. Niemax and K.-H. Weber, J. Phys. B: Atom. Mol. Phys. **11**, L267 (1978).
[18] C. J. Lorenzen, K.-H. Weber, and K. Niemax, Opt. Commun. **33**, 271 (1980).
[19] M. S. O'Sullivan and B. P. Stoicheff, Can. J. Phys. **61**, 940 (1983).
[20] K.-H. Weber and C. J. Sansonetti, Phys. Rev. A **35**, 4650 (1987).
[21] L. R. Pendrill, D. Delande, and J. C. Gay, J. Phys. B: Atom. Mol. Phys. **12**, L603 (1979).
[22] J. M. Raimond, P. Goy, G. Vitrant, and S. Haroche, J. Phys. Colloques. **42**, C8 (1981).
[23] P. M. Stone, Phys. Rev. **127**, 1151 (1962).
[24] E. M. Anderson and V. A. Zilitis, Opt. Spectrosc. **16**, 211 (1964).
[25] L. Agnew and C. Summers, in *Proceedings of the Seventh International Conference on Phenomena in Ionized Gases, Belgrade, 1966*, Vol. II, edited by B. Perović and D. Tošić (Gradevinska Knjiga, Belgrade, Yugoslavia), p. 574.
[26] S. M. Gridneva and G. A. Kasobov, in *Proceedings of the Seventh International Conference on Phenomena in Ionized Gases, Belgrade, 1965*, Vol. II, edited by B. Perović and D. Tošić (Gradevinska Knjiga, Belgrade, Yugoslavia), p. 581.
[27] M. Fabry, J. Quant. Spectros. Radiat. Transfer **16**, 127 (1975).
[28] M. Fabry and J. R. Cussenot, Can. J. Phys. **54**, 836 (1976).
[29] J. Lahiri and S. T. Manson, Phys. Rev. A **33**, 3151 (1986).
[30] S. Tojo, T. Fujimoto, and M. Hasuo, Phys. Rev. A **71**, 012507 (2005).
[31] A. Nadeem, M. Nawaz, S. Hussain, S. A. Bhatti, and M. A. Baig, J. Phys. B: Atom. Mol. Phys. **38**, 867 (2005)
[32] S.-U. Haq, S. Mahmood, M. A. Kalyar, M. Rafiq, R. Ali, and M. A. Baig, Eur. Phys. J. D **44**, 439 (2007).
[33] D. C. Hanna, P. A. Kärkkäinen, and R. Wyatt, Opt. Quant. Elect. **7**, 115 (1975).
[34] C. E. Burkhardt, J. L. Libbert, Jian Xu, J. J. Leventhal, and J. D. Kelley, Phys. Rev. A **38**, 5949 (1988).
[35] L.-W. He, C. E. Burkhardt, M. Ciocca, J. J. Leventhal, and S. T. Manson, Phys. Rev. Lett. **67**, 2131 (1991).
[36] L.-W. He, C. E. Burkhardt, M. Ciocca, J. J. Leventhal, H.-L. Zhou, and S. T. Manson, Phys. Rev. A **51**, 2085 (1995).
[37] W. Mende, K. Bartschat, and M. Kock, J. Phys. B: At. Mol. Opt. Phys. **28**, 2385 (1995).
[38] Sami-ul-Haq, S. Mahmood, N. Amin, Y. Jamil, R. Ali, and M. A. Baig, J. Phys. B: Atom. Mol. Opt. Phys. **39**, 1587 (2006).
[39] M. Rafiq, S. Hussain, M. Saleem, M. A. Kalyar, and M. A. Baig, J. Phys. B: At. Mol. Opt. Phys. **40**, 2291 (2007).
[40] S. Hussain, M. Saleem, M. Rafiq, and M. A. Baig, Phys. Rev. A **74**, 022715 (2006).
[41] A. Z. Msezane, J. Phys. B: At. Mol. Opt. Phys. **16**, L489 (1983).
[42] A. Z. Msezane and S. T. Manson, Phys. Rev. A **29**, 1594 (1984).
[43] H. P. Saha, Phys. Rev. A **41**, 174 (1990).
[44] R. J. Rafac, C. E. Tanner, A. E. Livingston, and H. G. Berry, Phys. Rev. A **60**, 3648 (1999).
[45] NIST database [www.physics.nist.gov.] (2009).
[46] W. Mende and M. Kock, J. Phys. B: At. Mol. Opt. Phys. **29**, 655 (1996).
[47] S. Hussain, M. Saleem, and M. A. Baig, Phys. Rev. A **75**, 022710 (2007).
[48] S. U. Haq, M. A. Kalyar, M. Rafiq, R. Ali, N. K. Piracha, and M. A. Baig, Phys. Rev. A **79**, 042502 (2009).
[49] M. A. Kalyar, M. Rafiq, S. U. Haq, and M. A. Baig, J. Phys. B: At. Mol. Opt. Phys. **40**, 2307 (2007).
[50] M. A. Baig, S. Mahmood, R. Mumtaz, M. Rafiq, M. A. Kalyar, S. Hussain, and R. Ali, Phys. Rev. A **78**, 032524 (2008).